ROJ Radiation Oncology Journal

Original Article

pISSN 2234-1900 · eISSN 2234-3156
Radiat Oncol J 2024;42(4):319-329
https://doi.org/10.3857/roj.2024.00262

Reinforcing treatment and evaluation workflow of stereotactic ablative body radiotherapy for refractory ventricular tachycardia

Hojin Kim[1,*], Sangjoon Park[1,*], Jihun Kim[2], Jin Sung Kim[1], Dong Wook Kim[1], Nalee Kim[3], Jae-Sun Uhm[4], Daehoon Kim[4], Hui-Nam Pak[4], Chae-Seon Hong[1], Hong In Yoon[1]

[1]*Department of Radiation Oncology, Yonsei Cancer Center, Heavy Ion Therapy Research Institute, Yonsei University College of Medicine, Seoul, Republic of Korea*
[2]*Department of Radiation Oncology, Gangnam Severance Hospital, Yonsei University College of Medicine, Seoul, Republic of Korea*
[3]*Department of Radiation Oncology, Samsung Medical Center, Sungkyunkwan University School of Medicine, Seoul, Republic of Korea*
[4]*Division of Cardiology, Department of Internal Medicine, Severance Cardiovascular Hospital, Yonsei University College of Medicine, Seoul, Republic of Korea*

Received: April 5, 2024
Revised: May 31, 2024
Accepted: June 21, 2024

Correspondence:
Hui-Nam Pak
Department of Cardiology, Yonsei University College of Medicine, 50 Yonsei-ro, Seodaemun-gu, Seoul 03722, Republic of Korea.
Tel: +82-2-2228-8459
E-mail: HNPAK@yuhs.ac
ORCID:
https://orcid.org/0000-0002-3256-3620

Chae-Seon Hong
Department of Radiation Oncology, Yonsei Cancer Center, Yonsei University Health System, 50 Yonsei-ro, Seodaemun-gu, Seoul 03722, Republic of Korea.
Tel: +82-2-2228-8108
E-mail: CS.HONG@yuhs.ac
ORCID:
https://orcid.org/0000-0001-8704-0635

Hong In Yoon
Department of Radiation Oncology, Yonsei Cancer Center, Yonsei University Health System, 50 Yonsei-ro, Seodaemun-gu, Seoul 03722, Republic of Korea.
Tel: +82-2-2228-8110
E-mail: YHI0225@yuhs.ac
ORCID:
https://orcid.org/0000-0002-2106-6856

*These authors contributed equally to this work.

Purpose: Cardiac radioablation is a novel, non-invasive treatment for ventricular tachycardia (VT), involving a single fractional stereotactic ablative body radiotherapy (SABR) session with a prescribed dose of 25 Gy. This complex procedure requires a detailed workflow and stringent dose constraints compared to conventional radiation therapy. This study aims to establish a consistent institutional workflow for single-fraction cardiac VT-SABR, emphasizing robust plan evaluation and quality assurance.

Materials and Methods: The study developed a consistent institutional workflow for VT-SABR, including computed tomography (CT) simulation, target volume definition, treatment planning, robust plan evaluation, quality assurance, and image-guided strategy. The workflow was implemented for two patients with cardiac arrhythmia. Accurate target volume definition using planning CT images and electronic anatomical mapping was critical. A four-dimensional (4D) cone-beam CT (CBCT) and breath-hold electrocardiographic gated CT images reliably detected target motion.

Results: The resulting plans exhibited a conformity index greater than 0.7 and a gradient index around G4.0. Dose constraints for the planning target volume (PTV) aimed for 95% or higher PTV dose coverage, with a maximum dose of 200% or lower. However, one case did not meet the PTV dose coverage due to the proximity of the PTV to gastrointestinal organs. Plans adhered to dose constraints for organs at risk near the heart, but meeting constraints for specific cardiac sub-structures was challenging and dependent on PTV location.

Conclusion: The plans demonstrated robustness against respiratory motion and patient positional uncertainty through a robust evaluation function. The 4D and intra-fractional CBCT were effective in verifying target motion and setup stability.

Keywords: Ventricular tachycardia, Stereotactic body radiotherapy, Radiotherapy planning

Introduction

Ventricular tachycardia (VT), a critical cardiac arrhythmia, presents significant challenges in cardiovascular medicine [1]. VT can originate idiopathically or from myocardial substrates, such as premature ventricular contractions (PVCs), leading to re-entrant circuits. These circuits, often involving an isthmus of slow-conducting fibers, are influenced by the site of ventricular activation, impacting the electrocardiographic profile of VT [2]. Pathologic changes, including post-myocardial infarction or post-inflammatory scars, are common factors increasing the susceptibility to VT.

Implantable cardioverter-defibrillators (ICDs) have been pivotal in managing sudden cardiac death from VT since the late 1970s. By detecting and treating malignant ventricular arrhythmias, primarily through anti-tachycardia pacing or shocks, ICDs are effective in treating VT episodes. However, they do not prevent VT onset and can adversely affect quality of life. antiarrhythmic drugs and catheter ablation (CA) are standard treatments for VT. CA, particularly with radiofrequency energy, aims to disrupt re-entrant circuits or modify potential substrates [3-5]. Despite advancements, CA faces challenges, such as limited efficacy, side effects, and high recurrence rates. Furthermore, the recurrence post-CA exceeds fifty percent within the first 2 years [6-9]; this is particularly concerning for non-ischemic origin VTs.

For patients with refractory VTs unresponsive to or unsuitable for conventional therapies, novel approaches are being explored. Among these, stereotactic ablative body radiotherapy (SABR) is garnering attention [10-12]. SABR, delivering a high radiation dose (20–25 Gy) in a single fraction, is particularly beneficial for medically unstable patients or those with slow VT. Advanced noninvasive cardiac imaging—including magnetic resonance imaging and computed tomography (CT) combined with body-surface electrocardiographic imaging—is crucial for identifying myocardial scars and arrhythmogenic substrates, enabling the precise targeting of lesions. VT-SABR necessitates the integration of multimodal imaging data for accurate target localization, adherence to strict dose constraints for SABR, and comprehensive image-guided radiation therapy (IGRT) for a single treatment.

Our institution conducted its inaugural VT-SABR procedure in 2019, initially basing the treatment protocol and radiation therapy (RT) preparations on a clinical site with prior relevant experience. Long-term follow-ups demonstrated the effectiveness of SABR for VT patients, leading to two recent cases being assigned to this non-invasive radioablation treatment.

The primary objectives of this study were to establish a consistent institutional workflow and intensify secure evaluation and quality assurance (QA) procedures for the single-fractionated cardiac VT-SABR. The first aim encompassed the precise delineation of target volumes through the integration of multimodal imaging data, and adherence to strict dose constraints for SABR treatment planning. The second objective was specified by a robust plan evaluation process reflecting several uncertainties from respiratory movement and positional set-up of patients, thorough observation of pre-treatment mechanical QA procedure, and rigorous image guidance on intra-fractional basis.

Materials and Methods

1. Patient history

Case 1, with diabetes mellitus, was diagnosed with dilated cardiomyopathy (DCMP). An ICD was implanted in September 2017 and later upgraded to a cardiac resynchronization therapy defibrillator (CRT-D) in June 2019. Subsequently, the patient underwent radiofrequency CA for recurrent VT in January 2021, thrice in March 2022, and once more in October 2022. Additionally, the patient had a sympathectomy in July 2022. This patient, frequently experiencing PVCs and recent ICD shocks, was admitted for the management of recurrent VT and referred for VT-SABR.

Case 2, with hypertension and chronic kidney disease, was diagnosed with DCMP and had a CRT-D defibrillator implanted. The patient underwent coronary angiography in April 2018. For recurrent VT with episodes of degeneration into ventricular fibrillation, radiofrequency CA was performed in November 2021, July 2022, October 2022, and November 2022. Like the first patient, this individual also experienced frequent PVCs. Following over ten ICD shocks in two days, the patient was admitted for the management of recurrent VT and referred for VT-SABR.

Fig. 1 describes the entire procedure of VT-SABR applied to the two recent patients, which were specified in the subsequent sections.

2. CT simulation

Several CT imaging sequences were employed, encompassing four-dimensional (4D) CT and free-breathing three-dimensional (3D) CT scans without contrast enhancement, along with breath-hold electrocardiographic (ECG) gated contrast-enhanced CT images. These images underwent metal artifact reduction (MAR) procedures to minimize artifacts stemming from implanted cardiac devices like ICDs and stents within cardiac structures. The imaging process was conducted using a single CT simulator, the Canon One Prism by Canon Medical Systems Corporation in Tochigi, Japan. This system allowed for both ECG gating and respiratory gating for the 4D CT scans, followed by MAR operations. These images contributed to the precise target volume definition in VT-SABR. The con-

https://doi.org/10.3857/roj.2024.00262

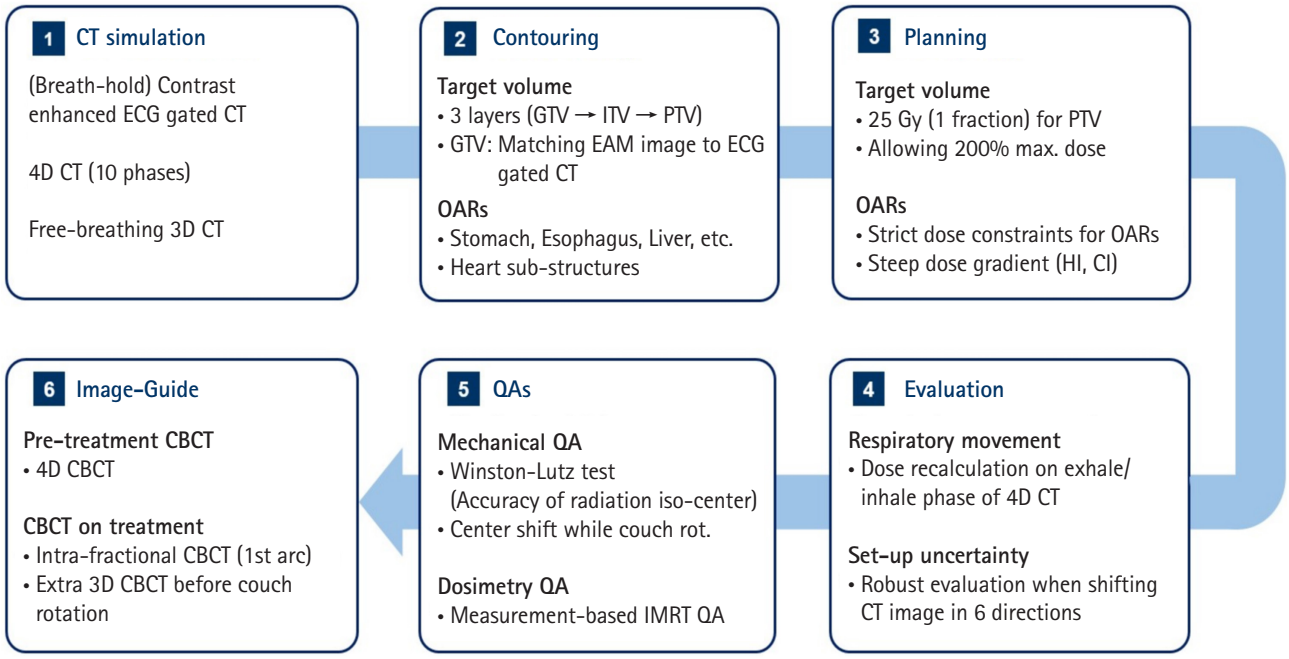

Fig. 1. Flowchart of VT-SABR established in our institution illustrating the steps from CT simulation to image-guided radiation therapy. VT, ventricular tachycardia; SABR, stereotactic ablative body radiotherapy; CT, computed tomography; ECG, electrocardiogram; 4D, four-dimensional; 3D, three-dimensional; GTV, gross tumor volume; ITV, internal target volume; PTV, planning target volume; EAM, electronic anatomical mapping; OAR, organ-at-risk; HI, homogeneity index; CI, conformity index; CBCT, cone-beam CT; QA, quality assurance; IMRT, intensity modulated radiation therapy.

trast-enhanced cardiac CT scans specifically focused on capturing cardiac movement during breath-holding, serving as an anatomical reference for delineating target volumes. These scans were compared against electronic anatomical mapping (EAM) or electrocardiographic images acquired during CA procedures [13,14]. Additionally, the 4D CT images, comprising 10 respiratory phases, provided reference data for understanding respiratory motion, aiding in the delineation of the internal target volume (ITV). The free-breathing CT image was primarily acquired to aggregate contours of target volumes and organs-at-risk (OARs). This data was instrumental in subsequent treatment planning processes.

3. Delineation of target volume and OARs by multi-modal imaging data

The integration of multi-modal imaging data is crucial in delineating target volumes for VT-SABR, aligning with the recommendations in the International Commission on Radiation Units and Measurements (ICRU) 62 [15]. The target volume for VT-SABR involves three layers: gross tumor volume (GTV), ITV, and planning target volume (PTV). Importantly, as stated in the preceding section, the free-breathing CT image was the reference image for delineations of target volumes and OARs. GTV referenced ECG-gated CT images with the EAM image, visualizing the activation map associated with the VT source using 3D cardiac imaging [16-19] obtained through the CARTO system (Johnson & Johnson MedTech, New Brunswick, NJ, USA) by cardiac electrophysiologists. On the cardiac gating CT images, the activated regions were identified as the GTV, as depicted in Fig. 2, showcasing the correlation between GTV contours, and activated regions in two recent VT-SABR cases at our institution. This contouring information was further aligned with the exhale phase of the 4D CT via image registration to ECG-gated CT. In this alignment, there was no further registration needed as the images were acquired at the same CT scanning session. Using a deformable image registration algorithm on MIM software (https://www.mimsoftware.com/), the target volumes in the exhale phase were extended to other phases, establishing the ITV, which was defined in the primary free-breathing 3D CT image. Alongside 4D CT, we utilized all phase images from ECG-gated CT to ensure the target in the planning CT was encompassed within the ITV. PTV was established by expanding the ITV by 5 mm, considering the spatial orientation of OARs. This contouring process was then transferred to the free-breathing 3D CT image for subsequent treatment planning.

Precise delineation of OARs was crucial for VT-SABR due to the proximity of several critical organs—including the esophagus, stomach, and great vessels—to cardiac structures. Given that high doses of radiation were administered to certain parts of the heart, the dose constraints for treatment planning had to account for

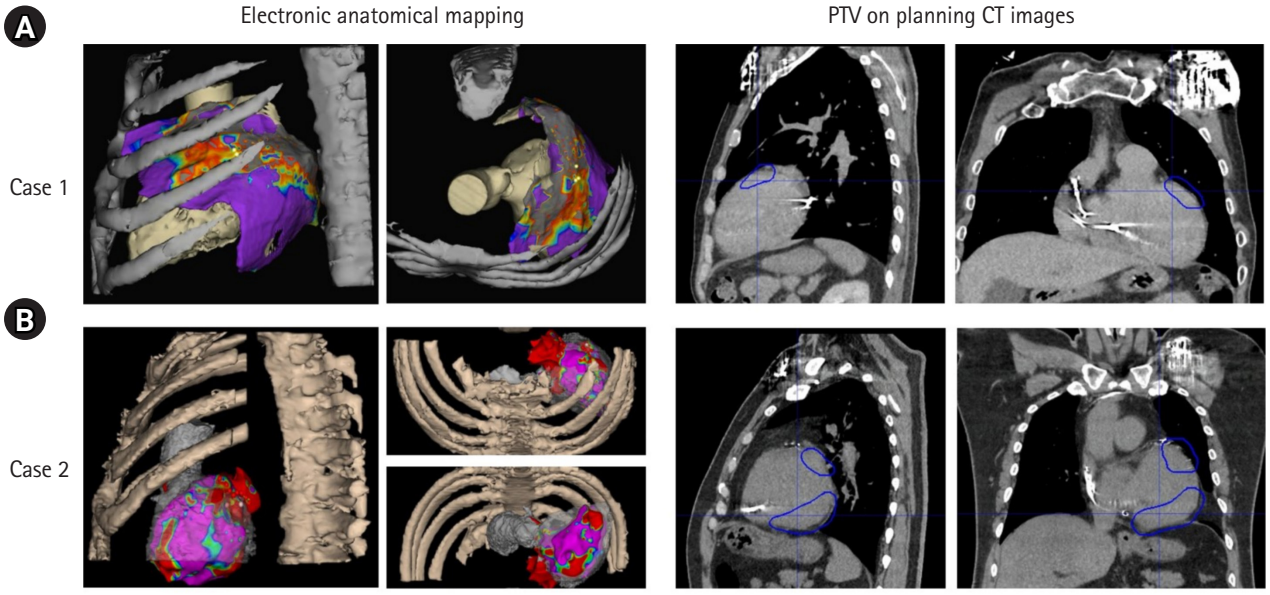

Fig. 2. Target volume delineation (right column) with reference to the regions activated in electronic anatomical mapping for two cases: (A) case 1 and (B) case B. PTV, planning target volume; CT, computed tomography.

cardiac sub-structures. A deep learning-based software (Oncosoft, Seoul, Korea) automatically segmented critical organs—including the esophagus, stomach, liver, lung, and cardiac sub-structures—on the free-breathing 3D CT images. This segmentation was refined by radiation oncologists. The relative positioning of critical organs, such as the stomach and esophagus, complicated treatment planning and influenced the choice of beam arrangement (coplanar vs. non-coplanar).

4. Treatment planning

The reference CT image for treatment planning was the free-breathing 3D CT images. All VT patients underwent SABR treatment in a single fraction at a prescribed dose of 25 Gy for the PTV, allowing for a maximum dose of 200% of the prescribed dose (50 Gy). Dose constraints for critical organs such as the spinal cord, lung, liver, esophagus, and stomach adhered to guidelines established in a prior study [20]. However, for the heart and its sub-structures, dose constraints varied depending on PTV location. For these, the median dose outlined in the same study [20] was referenced during the treatment planning process. RayStation v11.1 (RaySearch Laboratories, Stockholm, Sweden) was utilized for treatment planning. The chosen treatment modality, the Versa HD conventional C-arm linear accelerator (Elekta AB, Stockholm, Sweden), was employed for VT-SABR.

The determination of beam arrangement (i.e., a coplanar or non-coplanar scheme) critically influences treatment efficiency and subsequent processes like evaluation, QA, and image guidance during actual treatment. As anticipated, while the non-coplanar arrangement with couch rotation promised greater plan quality and robustness, it also increased the time required for actual treatment, QA, and image guidance. Therefore, the coplanar treatment strategy was preferred. However, for the second case where the stomach and esophagus were proximal to the PTV, the non-coplanar scheme was used.

The quality of the resulting treatment plans was evaluated using parameters such as PTV dose coverage (the volume of PTV receiving more than the prescribed dose), conformity index (CI), and gradient index (GI) calculated using the following Equations (1) and (2).

$$\text{CI} = \frac{V_{PTV,100\%}}{V_{PTV}} \cdot \frac{V_{PTV,100\%}}{V_{100\%}}, \tag{1}$$

$$\text{GI} = \frac{V_{50\%}}{V_{100\%}} \left(\text{GI}_{\text{low}} = \frac{V_{25\%}}{V_{100\%}}, \text{GI}_{\text{High}} = \frac{V_{75\%}}{V_{100\%}} \right). \tag{2}$$

where V_{PTV} means the volume of PTV, and $V_{PTV,100\%}$ is the volume of PTV receiving 100% of the prescribed dose. And $V_{100\%}$, $V_{75\%}$, $V_{50\%}$, and $V_{25\%}$ represent the volumes of the entire body receiving 100%, 75%, 50%, and 25% of the prescribed dose, respectively.

5. QAs and robust evaluation

The stringent dose constraints involved in SABR require mechanical and dosimetric accuracy [21]. To ensure this, various QA procedures were implemented. The Winston-Lutz test was conducted to verify the alignment of radiation and mechanical iso-centers, even during

 https://doi.org/10.3857/roj.2024.00262

couch rotation. Furthermore, the center shift caused by couch rotation was measured, setting a tolerance of < 1 mm for both criteria. In addition to mechanical QA, pre-treatment, patient-specific intensity-modulated radiation therapy (IMRT) QA was conducted using the ArcCheck system (Sun Nuclear Corporation, Melbourne, FL, USA). This assessed dose distribution accuracy through gamma passing rates and measured point doses at the center of ArcCheck using an A1SL ionization chamber (Standard Imaging Inc., Middleton, WI, USA).

Plan robustness was assessed using RayStation treatment planning system evaluating resilience against respiratory motion and patient setup uncertainty. The optimized treatment plan on the free-breathing CT image underwent dose recalculation on end-of-exhale and end-of-inhale CT images derived from 4D CT scans with the same RT plan data. Accounting for patient setup uncertainty in all dimensions, a robust evaluation function provided by RayStation was employed and assessed by dose-volume histograms (DVHs) and dose distributions.

6. Image-guidance

Like conventional IMRT and SABR treatments, volumetric cone-beam CT (CBCT) scans were conducted before treatment for image guidance. The Versa HD C-arm linear accelerator used for VT-SABR provided 4D CBCT functionality before treatment to confirm respiratory movement similarity with planning CT and intra-fractional CBCT during beam-on time to monitor patient position consistency. Before treatment initiation, 4D CBCT scans were matched. Intra-fractional CBCT was performed during the initial arc delivery of the volumetric modulated arc therapy plan. For non-coplanar plans, the same procedure was followed, with additional CBCT scans conducted after completing coplanar arcs and before couch rotation for the non-coplanar arc.

Results

1. Planning results

Table 1 specifies the treatment plans for the two cases. Both used the arc-based IMRT treatment scheme with 6 MV flattening filter-free mode. The first case used three arcs with 10900 monitor unit (MU), which was treated by a coplanar beam arrangement. The second case had multiple OARs—the stomach, and esophagus—proximal to the target volume, which affected the non-coplanar

Table 1. VMAT planning information for cases 1 and 2

	Case 1	Case 2
Beam arrangement	Coplanar	Non-coplanar
Energy/mode	6 MV/FFF	6 MV/FFF
MU	10900.5	28474.7
Number of arcs	3	5
PTV (mL)	18.18	247.57

VMAT, volumetric modulated arc therapy; MU, monitor unit; PTV, planning target volume; MV, megavoltage; FFF, flattening filter free.

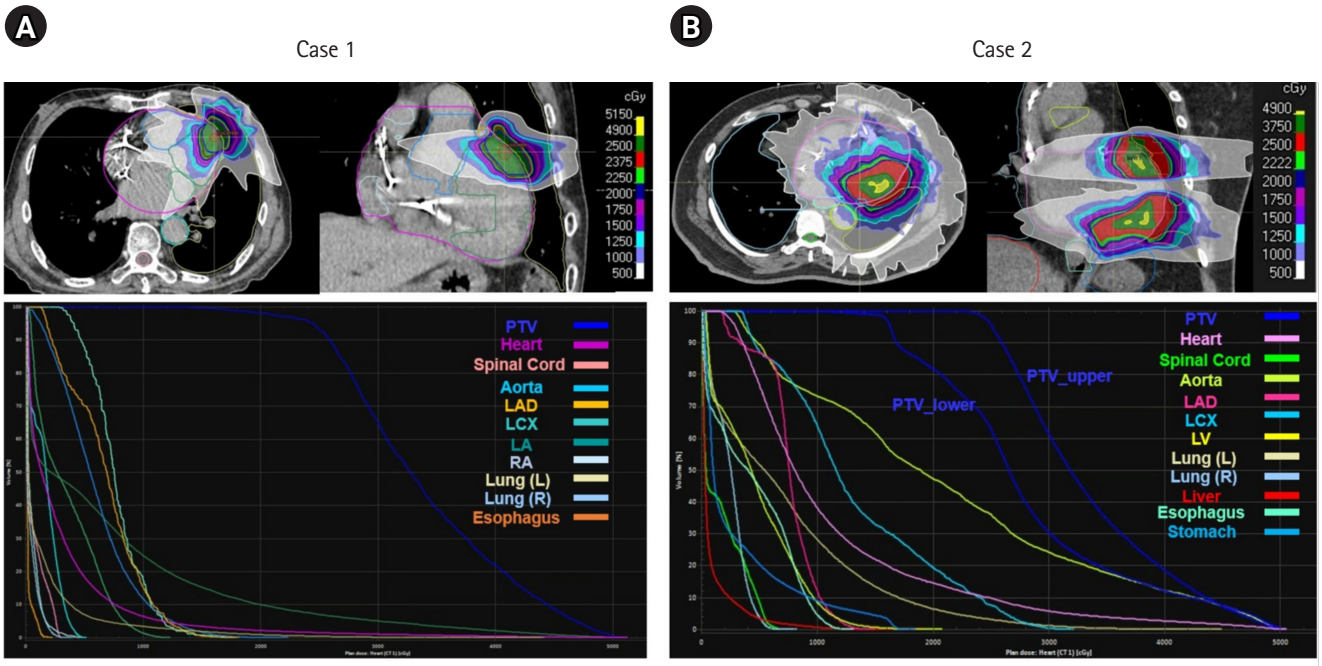

Fig. 3. (Top row) Dose distributions, (Bottom row) dose-volume histograms for PTV and organs-at-risk produced from treatment plans of (A) case 1 and (B) case 2. PTV, planning target volume; LAD, left anterior descending artery; LCX, left circumflex artery; LV, left ventricle; L, left; R, right; LA, left atrium; RA, right atrium.

Table 2. Dose constraints and results from the optimized treatment plans for cases 1 and 2

Structure	Dose constraints	Case 1	Case 2
Target volume			
PTV	$V_{100\%}$ ≥ 95 (%)	94.57	73.52
	D_{max} (Gy)	49.69	49.43
	CI	0.79	0.72
	GI	4.36	4.07
	GI_{low}	13.24	15.87
	GI_{high}	1.93	1.83
OARs (excluding cardiac adjacent structures)			
Spinal cord	D_{max} ≤ 14 (Gy)	2.98	6.73
	$D_{1.2mL}$ ≤ 8 (Gy)	2.51	5.49
Esophagus	D_{5mL} ≤ 15.4 (Gy)	0.25	9.86
Stomach	D_{5mL} ≤ 22 (Gy)	-	16.59
Lung total	RV_{7Gy} ≤ 1,500 (mL)	70.54	423.22
Liver	RV_{11Gy} ≤ 700 (mL)	-	3.49
OARs (Including heart-related structures)			
Heart (excluding PTV)	$D_{50\%}$ (Gy)	1.31	7.23
Aorta	D_{max} ≤ 20.0 (Gy)	5.06	19.82
Left coronary artery	D_{max} ≤ 14.0 (Gy)	14.05	**31.54**
Left atrium	D_{max} ≤ 4.4 (Gy)	**12.05**	-[a]

PTV, planning target volume; $V_{100\%}$, percent volume receiving 100% of the prescribed dose at the structure; CI, conformity index; GI, gradient index; GI_{low}, GI for low dose; GI_{high}, GI for high dose; OAR, organ-at-risk; RV, reverse volume; D_{max}, maximum dose irradiated to the structure; $D_{1.2mL}/D_{5mL}$, dose irradiated to 1.2ml/5ml of the structure; RV_{7Gy}/RV_{11Gy}, normal tissue volume receiving < 7 Gy/11 Gy; $D_{50\%}$, dose irradiated to 50% of volume of the structure.
Numbers in bold indicate violations in dose constraints.
[a]Target overlapped with the left atrium.

beam arrangement. Besides the arrangement, the PTV volume being greater than in the first case required a larger MU (28474 MU) with more arcs (5 > 3). The first three arcs with a coplanar setting delivered doses to the upper target of the PTV, while the remaining two arcs with a couch rotation of 5° delivered doses to the lower volume of the PTV. Fig. 3 illustrates the dose distributions and DVHs of PTV and OARs generated by the treatment plans. The treatment plan yielded inhomogeneous dose distributions inside the PTV, wherein the PTV coverage was reduced in Case 2 due to the lower parts of the PTV. In Case 1, most critical organs received low doses of radiation since the PTV volume was small and no critical organs were adjacent to the target volume. However, many of the cardiac substructures, as well as the esophagus and stomach, received high doses of radiation due to the PTV location and volume.

Table 2 lists the planning results of the two cases for PTV and OARs along with dose constraints applied. The PTV dose coverage of the first case almost met the criterion expected to be greater than 95%, whereas the second case did not satisfy the criterion to minimize the dose irradiated to the stomach and esophagus adjacent to the lower part of the PTV. The maximum allowed dose for both cases was 200% of the prescribed dose for the steep-dose fall-off gradient, which resulted in GIs of 4.36 and 4.07. The CIs for the two cases were 0.79 and 0.72, wherein the lower CI in Case 2 was mainly due to the decrease in PTV coverage (73.5%) as seen in Equation (2). The OARs—excluding cardiac adjacent structures such as the spinal cord, esophagus, stomach, lung, and liver—met the dose constraints successfully. The stomach and liver in the first case were not involved since the PTV was defined in the upper portion of the heart. Contrarily, for the heart and its sub-structures, the resultant plans did not completely satisfy the dose constraints.

Table 3. Dose constraints and results from the optimized treatment plans for cases 1 and 2

QA category	Case 1	Case 2
Mechanical QA (mm)		
Couch rotation	-[a]	< 0.50
Winston-Lutz	0.46	0.89
IMRT QA (%)		
Point dose	0.42	-2.90
GPR (3%/3 mm)	97.40	91.80

QA, quality assurance; IMRT, intensity-modulated radiation therapy; GPR, gamma passing rate.
[a]Coplanar arrangement.

https://doi.org/10.3857/roj.2024.00262

The treatment plan for Case 1 violated the dose constraint for the left atrium, and the plan for Case 2 did not satisfy the constraint for the left coronary artery and left atrium. Meeting the dose constraints for the cardiac sub-structures depended on the location of the target volume.

2. QA and evaluation

Table 3 summarizes the QA tasks performed on the day for the single-fractionated VT-SABR. The coincidence between mechanical and radiation iso-centers was smaller than the tolerance (1 mm for SABR). The difference grew when the couch rotation was involved. The magnitude of center shift from couch rotation, which was conducted only for the non-coplanar RT case, was less than 0.5 mm. In dosimetry, a patient-specific IMRT QA performed with ArcCheck led to point dose differences of 0.4% and -2.9% and gamma passing rates of 97.4% and 91.8%. The IMRT dosimetry error was slightly worse when the beam arrangement was non-coplanar.

The robustness of the resultant plan was also evaluated for the respiratory motion and patient set-up uncertainties. For respiratory motion, the dose re-calculated on CT images during inhalation and exhalation resulted in the DVHs (solid) in Fig. 4, relative to the DVHs (dashed) on the reference CT images. The dose distributions were not perturbed severely due to the respiratory motion, while the under-dosage on the PTV occurred in the exhale and inhale phases for Cases 1 and 2, respectively. For Case 2, cardiac adjacent structures, such as the aorta and the left ventricle (LV), were underdosed. The dosimetry impact from patient position uncertainty was evaluated using RayStation by robust evaluation that imposed the positional uncertainty on the CT images in six different scenarios, wherein the extent of uncertainty was assumed to be 1 mm. Fig. 5 compares the DVHs (solid) in six different scenarios relative to the DVHs (dashed) from the original plans for Cases 1 and 2. In Case 1, dosimetry did not change significantly except for the left anterior descending (LAD) and left circumflex (LCX) arteries. Despite the variations depending on the patient position, the dose of radiation to the LAD and LCX was quite low. For Case 2, the variations in dosimetry were enlarged when the patient set-up was perturbed craniocaudally. The dose irradiated to the LV was similar or slightly larger in the superior and inferior set-up errors. However, the dose of radiation to PTV decreased when the patient set-up error was imposed inferiorly.

3. Off-line review of patient set-up

IGRT was performed by leveraging the special functions of the Ver-

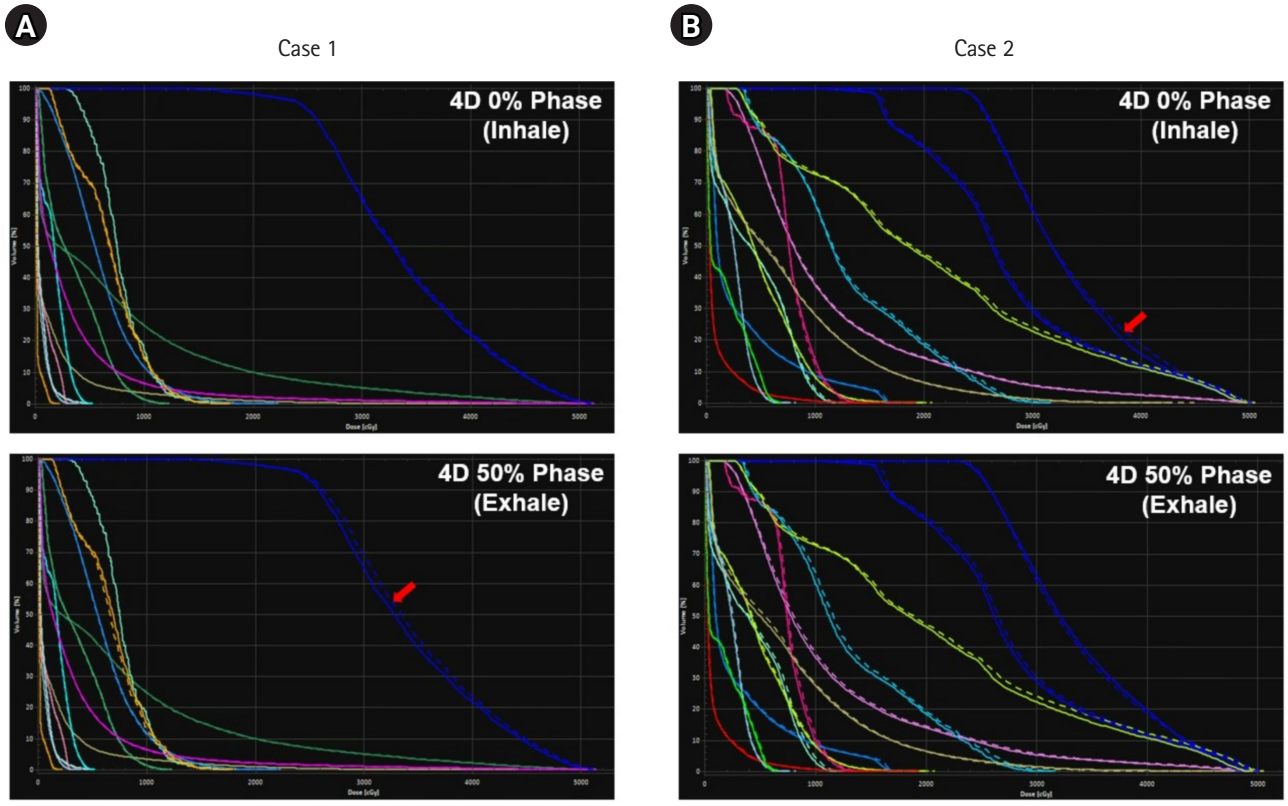

Fig. 4. Dose volume histograms from the dose recalculated on the inhale (top) and exhale (bottom) phases of the four-dimensional (4D) computed tomography images investigating the degree of dosimetry impact from the respiratory motion: (A) case 1 and (B) case 2.

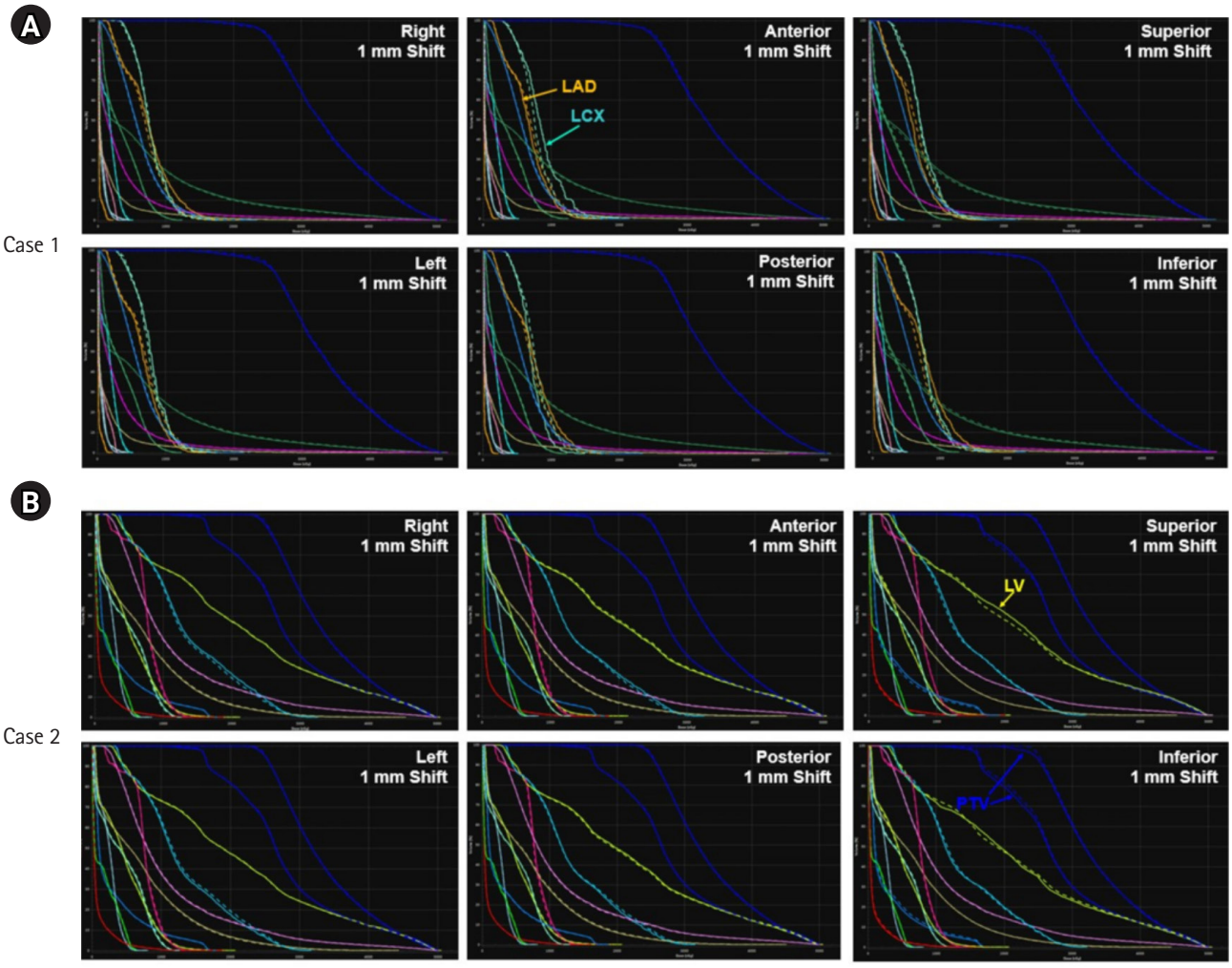

Fig. 5. Robust evaluation of patient set-up uncertainty: comparing DVHs (solid) from patient set-up errors in six different scenarios (1 mm shift in each direction) to DVHs (dashed) from the original plan: (A) case 1 and (B) case 2. DVH, dose volume histogram; LAD, left anterior descending artery; LCX, left circumflex artery; LV, left ventricle; PTV, planning target volume.

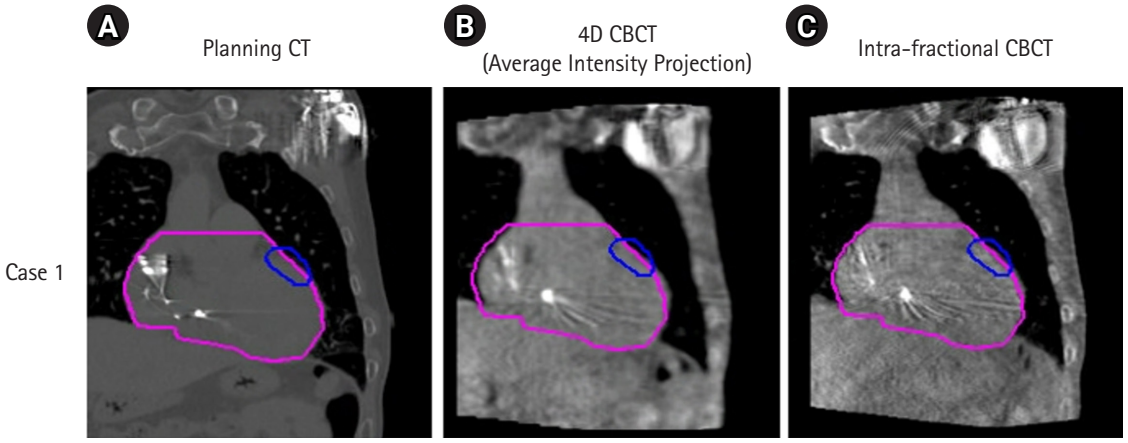

Fig. 6. Cone-beam computed tomography (CBCT) image acquisitions for image-guided radiation therapy for ventricular tachycardia stereotactic ablative body radiotherapy of the first patient case: (A) planning CT image, (B) 4D CBCT image, and (C) intra-fractional CBCT image. 4D, four-dimensional.

https://doi.org/10.3857/roj.2024.00262

sa HD linear accelerator. Fig. 6 illustrates the 4D and intra-fractional CBCT images acquired and matched against the planning CT images of the first patient case. Before the first arc delivery, the 4D CBCT was acquired such that the PTV covered the respiratory motion of the patient, as shown in Fig. 6B. The intra-fractional CBCT was also acquired during the first arc dose delivery to examine if the patient set-up was well maintained during treatment, as seen in Fig. 6C. The catheters embedded in the cardiac structures acted as markers when matching the images.

4. Clinical treatment outcome

Post-treatment, the first patient reported no significant adverse effects in the outpatient follow-up. Approximately three weeks following SABR, the patient experienced VT episodes at a similar rate to that before the treatment, averaging about 5 per week. However, in the 2 months following this period, no notable episodes occurred. The follow-up for this patient continued for seven months.

The second patient did not experience any VT episodes during the follow-up. However, one month after treatment, the patient reported grade 1 epigastric pain in the outpatient. This patient also reported feelings of fatigue post-treatment. Apart from these events, no other complications or symptoms were noted. The follow-up for the second patient lasted for 6 months.

Discussion and Conclusion

Cardiac radioablation is a potent treatment alternative for VT. However, the execution of VT-SABR has been limited due to the required specialized imaging and treatment facilities, proficient clinical workforce, and interdisciplinary collaboration. This study primarily focuses on establishing and disseminating a systematic clinical workflow for VT-SABR that aligns with our institutional RT procedures.

Crucial points for each step, depicted in Fig. 1, were highlighted. The CT simulation containing a series of CT datasets was preferred to be performed at the same session since the ECG-gated, 4D, and planning CTs were co-registered for the target volume definition. Furthermore, as part of the inter-departmental collaboration, both cardiologists and radiation oncologists had to be involved in the target volume for the precise target volume definition. The treatment planning must consider the locations of OARs and heart sub-structures in relation to the target volume when meeting the strict dose constraints of SABR. Due to the dose constraints of some of the critical organs, the PTV coverage might be sacrificed. Non-coplanar beam arrangement may be considered at the expense of treatment efficiency. The resultant treatment plan was assessed by robust evaluation with variations in respiratory motion and positional uncertainty, which assist image-guiding strategies during the actual treatment. In the image guiding step, 4D and intra-fractional CBCT were actively adopted to monitor the respiratory movement relative to the ITV contour.

The resultant plans met the dose constraints required for the OARs, excluding the cardiac adjacent structures, for which the resultant plan violated the dose requirements. This was somewhat inevitable given the PTV locations. The plan was robust under respiratory motion, implying that the PTV extended from the ITV considering the whole phases from the 4D CT was sufficient to conceal the respiratory movement. Furthermore, the dose of radiation to the OARs was too little to be affected by the respiratory motion. The patient positional uncertainty, however, led to a slightly greater influence on the dose distribution. For both cases, the dosimetry impact from position uncertainty was enlarged in craniocaudal directions, which indicated that the CBCT image matching to the planning CT would require more care in superior and inferior directions.

This study had certain limitations. The cardiac radioablation treatment in this study was conducted using the C-arm linear accelerator, but our facility has a non-coplanar, non-isocentric treatment modality (CyberKnife M6; Accuracy, Sunnyvale, CA, USA). Previous studies [22-25] have compared the quality of plans optimized for different treatment modalities, which claimed that the CyberKnife resulted in superior plan quality at the cost of the dose delivery time. Furthermore, aside from the ITV-based management used in this study, different motion management approaches exist, including fiducial tracking (available in CyberKnife) and gating-based methods. Such motion management techniques may substantially contribute to reducing the PTV target volume while sacrificing the prolonged treatment time. The points stated previously were greatly associated with delivery efficiency. Although advanced techniques and modalities might improve the quality of treatment theoretically, the treatment time might be doubled. Considering patients experiencing cardiac arrhythmias, trade-offs associated with delivery efficiency and plan quality must be considered when establishing the workflow. Finally, the target volume definition relied heavily on the activated regions in the EAM images. The EAM images provided by CARTO were unable to be co-registered with the CT images since they did not support the DICOM format. Several recent studies [16,18,19] concentrated on improving the precision of the target volume definition based on the EAM images throughout the file format transformation and open-source software. The accuracy of the target volume definition can be enhanced using such methodologies.

The clinical workflow for the VT-SABR was established and applied to actual treatment. Special care was taken for the precise

target definition, and treatment planning. With a focus on patient safety, procedures including patient-specific plan evaluation, mechanical QA procedure, and intra-fractional IGRT were effectively conducted. It was demonstrated that the resultant treatment plans were robust even with respiratory motion and patient position uncertainty. Also, the volumetric images reconstructed during RT treatment were well aligned with the planning CT images.

Statement of Ethics

This study was conducted in accordance with the principles of the Declaration of Helsinki and received approval from the Institutional Review Board of Severance Hospital (No. 4-2023-1558).

Conflict of Interest

No potential conflict of interest concerning this article has been disclosed.

Funding

This work was supported by the National Research Foundation of Korea (NRF) grant funded by the Korean government (MSIT) (No. RS-2023-00279682) and a faculty research grant from Yonsei University College of Medicine for (No. 6-2022-0174).

Author Contributions

Conceptualization, HIY, CSH, HNP; Investigation and methodology, HJK, SP; Project administration, HIY, CSH; Resources, HK, SP, JK, JSK, DK, NK, JSU, DK HNP, CSH, HIY. Supervision, HIY, HNP; Writing of original draft, HJK, CSH, SP; Writing of the review and editing, HIY, HNP; Formal analysis, HJK.

Data Availability Statement

The data supporting the conclusions of this study can be obtained from the corresponding author upon a reasonable request.

References

1. John RM, Tedrow UB, Koplan BA, et al. Ventricular arrhythmias and sudden cardiac death. Lancet 2012;380:1520–9.
2. Jumeau R, Ozsahin M, Schwitter J, et al. Stereotactic radiotherapy for the management of refractory ventricular tachycardia: promise and future directions. Front Cardiovasc Med 2020;7:108.
3. Al-Khatib SM, Stevenson WG, Ackerman MJ, et al. 2017 AHA/ACC/HRS Guideline for management of patients with ventricular arrhythmias and the prevention of sudden cardiac death: a report of the American College of Cardiology/American Heart Association Task Force on Clinical Practice Guidelines and the Heart Rhythm Society. J Am Coll Cardiol 2018;72:e91–220.
4. Shivkumar K. Catheter ablation of ventricular arrhythmias. N Engl J Med 2019;380:1555–64.
5. Santangeli P, Muser D, Maeda S, et al. Comparative effectiveness of antiarrhythmic drugs and catheter ablation for the prevention of recurrent ventricular tachycardia in patients with implantable cardioverter-defibrillators: a systematic review and meta-analysis of randomized controlled trials. Heart Rhythm 2016;13:1552–9.
6. Calkins H, Epstein A, Packer D, et al. Catheter ablation of ventricular tachycardia in patients with structural heart disease using cooled radiofrequency energy: results of a prospective multicenter study. Cooled RF Multi Center Investigators Group. J Am Coll Cardiol 2000;35:1905–14.
7. Carbucicchio C, Santamaria M, Trevisi N, et al. Catheter ablation for the treatment of electrical storm in patients with implantable cardioverter-defibrillators: short- and long-term outcomes in a prospective single-center study. Circulation 2008;117:462–9.
8. Stevenson WG, Wilber DJ, Natale A, et al. Irrigated radiofrequency catheter ablation guided by electroanatomic mapping for recurrent ventricular tachycardia after myocardial infarction: the multicenter thermocool ventricular tachycardia ablation trial. Circulation 2008;118:2773–82.
9. Tanner H, Hindricks G, Volkmer M, et al. Catheter ablation of recurrent scar-related ventricular tachycardia using electroanatomical mapping and irrigated ablation technology: results of the prospective multicenter Euro-VT-study. J Cardiovasc Electrophysiol 2010;21:47–53.
10. Cuculich PS, Schill MR, Kashani R, et al. Noninvasive cardiac radiation for ablation of ventricular tachycardia. N Engl J Med 2017;377:2325–36.
11. Neuwirth R, Cvek J, Knybel L, et al. Stereotactic radiosurgery for ablation of ventricular tachycardia. Europace 2019;21:1088–95.
12. Lloyd MS, Wight J, Schneider F, et al. Clinical experience of stereotactic body radiation for refractory ventricular tachycardia in advanced heart failure patients. Heart Rhythm 2020;17:415–22.
13. Cuculich PS, Zhang J, Wang Y, et al. The electrophysiological cardiac ventricular substrate in patients after myocardial infarction: noninvasive characterization with electrocardiographic imaging. J Am Coll Cardiol 2011;58:1893–902.
14. Lydiard PGDip S, Blanck O, Hugo G, O'Brien R, Keall P. A review of cardiac radioablation (CR) for arrhythmias: procedures, technology, and future opportunities. Int J Radiat Oncol Biol Phys

2021;109:783–800.
15. International Commission on Radiation Units and Measurements. ICRU Report 62: Prescribing, recording and reporting photon beam therapy (Supplement to ICRU Report 50). J ICRU 1999;os-32:1–52.
16. Hohmann S, Henkenberens C, Zormpas C, et al. A novel open-source software-based high-precision workflow for target definition in cardiac radioablation. J Cardiovasc Electrophysiol 2020;31:2689–95.
17. Boda-Heggemann J, Blanck O, Mehrhof F, et al. Interdisciplinary clinical target volume generation for cardiac radioablation: multicenter benchmarking for the RAdiosurgery for VENtricular TAchycardia (RAVENTA) Trial. Int J Radiat Oncol Biol Phys 2021;110:745–56.
18. Rigal L, Benali K, Barre V, et al. Multimodal fusion workflow for target delineation in cardiac radioablation of ventricular tachycardia. Med Phys 2024;51:292–305.
19. Brett CL, Cook JA, Aboud AA, Karim R, Shinohara ET, Stevenson WG. Novel Workflow for conversion of catheter-based electroanatomic mapping to DICOM imaging for noninvasive radioablation of ventricular tachycardia. Pract Radiat Oncol 2021;11:84–8.
20. Knutson NC, Samson PP, Hugo GD, et al. Radiation therapy workflow and dosimetric analysis from a phase 1/2 trial of noninvasive cardiac radioablation for ventricular tachycardia. Int J Radiat Oncol Biol Phys 2019;104:1114–23.
21. Klein EE, Hanley J, Bayouth J, et al. Task Group 142 report: quality assurance of medical accelerators. Med Phys 2009;36:4197–212.
22. Weidlich GA, Hacker F, Bellezza D, Maguire P, Gardner EA. Ventricular tachycardia: a treatment comparison study of the cyberknife with conventional linear accelerators. Cureus 2018;10:e3445.
23. Bonaparte I, Gregucci F, Surgo A, et al. Linac-based STereotactic Arrhythmia Radioablation (STAR) for ventricular tachycardia: a treatment planning study. Jpn J Radiol 2021;39:1223–8.
24. Wang L, Fahimian B, Soltys SG, et al. Stereotactic arrhythmia radioablation (STAR) of ventricular tachycardia: a treatment planning study. Cureus 2016;8:e694.
25. Kluge A, Ehrbar S, Grehn M, et al. Treatment planning for cardiac radioablation: multicenter multiplatform benchmarking for the RAdiosurgery for VENtricular TAchycardia (RAVENTA) Trial. Int J Radiat Oncol Biol Phys 2022;114:360–72.